# Intertube Coupling in Ropes of Single-Wall Carbon Nanotubes

H. Stahl,[1] J. Appenzeller,[1] R. Martel,[2] Ph. Avouris,[2] and B. Lengeler[1]
[1]*2. Physikalisches Institut, RWTH Aachen, D-52056 Aachen, Germany*
[2]*IBM T. J. Watson Research Center, Yorktown Heights, New York 10598*
(Received 24 March 2000)

We investigate the coupling between individual tubes in a rope of single-wall carbon nanotubes using four probe resistance measurements. By introducing defects through the controlled sputtering of the rope we generate a strong nonmonotonic temperature dependence of the four terminal resistance. This behavior reflects the interplay between localization in the intentionally damaged tubes and coupling to undamaged tubes in the same rope. Using a simple model we obtain the coherence length and the coupling resistance. The coupling mechanism is argued to involve direct tunneling between tubes.

PACS numbers: 73.61.Wp, 72.15.Rn, 72.80.Rj, 73.40.Gk

The unique structural and electronic properties of carbon nanotubes make them interesting objects for basic science study as well as applications. The relation between their geometry and electronic structure is of particular interest. Semiconducting or metallic behavior is possible depending on tube diameter and chirality [1]. Based on their unique properties, several applications in electronics have been proposed and some, such as field effect transistors [2,3] and diodes [4], have already been demonstrated. While the electronic structure of individual tubes has been characterized using scanning tunneling spectroscopy and found to be in agreement with the theoretical predictions [5], the interaction between tubes in ropes has received much less attention. Some studies have concluded that the coupling between tubes must be weak [6], but few attempted to directly measure this interaction [4,7]. Thus, most of the applications rely on single tubes bridging metal contacts [2,8]. However, the extensive use of nanotubes in future nanoelectronics would also require a knowledge of the tube-tube electronic coupling.

Here, we present a novel approach that allows us to determine the electrical coupling between tubes in a rope using four terminal transport measurements. The ropes are self-assembled bundles of carbon nanotubes, in which the tubes line up parallel to each other. The tubes in our ropes have diameters close to 1.4 nm and form a regular triangular lattice with a lattice constant of $d_0 = 1.7$ nm [9]. Both semiconducting and metallic tubes are present in a rope in a random distribution. In our experiment, the ropes were dispersed in dichloroethane using mild sonication, followed by several stages of centrifugation. The purified nanotube ropes were dispersed on an oxidized Si substrate and gold electrodes were subsequently fabricated on top of the ropes (see Fig. 1a). The key feature in our investigation involves a sputtering of the rope before deposition of the electrodes by an $Ar^+$ ion beam at an energy of 500 eV. The purpose of the sputtering is to introduce defects into the top nanometers of the rope. As will be shown later, this will enable us to vary the path taken by the electric current in a well-defined manner.

In order to estimate the extent of the sputter damage, a Monte Carlo simulation was performed [10]. The simulation was done on a carbon target with the mass density of nanotube ropes. The ions were found to produce about eight carbon vacancies per ion in a range $6 \pm 1$ nm deep into the rope (cf. Fig. 1b). From our sputter conditions ($Ar^+$ flux $\approx 1.5 \times 10^{15}$ $m^{-2}\,s^{-1}$ for 20 s) we infer a defect density of about one defect per 1000 atoms, which gives a distance of 5–10 nm between defects along the tubes. This defect density is high enough to have a significant

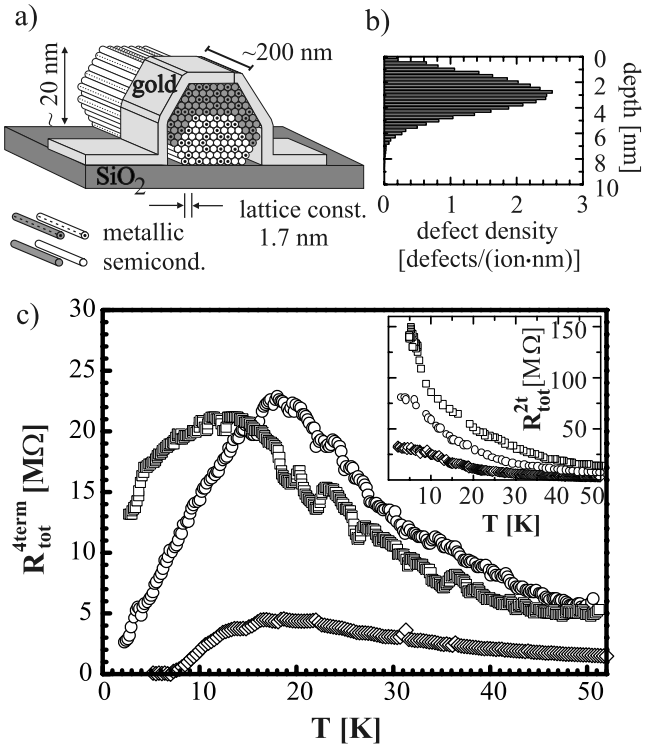


FIG. 1. Schematic of a section of a rope (a) together with a simulation of the distribution of the defects introduced by the sputter treatment (b). The shading marks the damaged tubes. Part (c) shows four (4t) and two (2t) terminal resistances versus temperature for three different samples.

 0031-9007/00/85(24)/5186(4)$15.00 

influence on the electrical properties of the tubes, while at the same time, it is low enough for the damaged tubes to preserve their structural integrity. The damage in the upper part of the rope is confined to the area directly underneath the gold contacts (note the shading in the schematic of the rope in Fig. 1a), while the main part of the rope between the electrodes was not exposed to the ion beam and is thus undamaged. Electronic transport in the damaged metallic tubes is strongly affected by the defects, while contributions from semiconducting tubes are negligible at the low temperatures used in the experiments (the typical band gap for semiconducting tubes of ~1.4 nm diameter is ~500 meV [1,5]).

The resistances were measured in the Ohmic regime using standard lock-in techniques while the sample was cooled in a $^4$He continuous flow cryostat with a base temperature of 1.5 K. We fully characterized 13 rope samples. Typical results of $R$ vs $T$ curves are presented in Fig. 1c. The two terminal (2t) resistances were found to increase with decreasing temperature. On the other hand, the four terminal (4t) measurements showed a pronounced resistance maximum at temperatures around 20 K in all of the samples we made. This behavior is caused by the damage introduced by sputtering. As a comparison, a 4t measurement of an undamaged rope is shown in the lower inset of Fig. 2. In this case, we observe a decrease in resistance with decreasing temperature over the whole temperature range. Thus, the undamaged ropes show a metallic behavior as is expected for ropes consisting, at least in part, of metallic tubes [11]. It is important to note the very different values of the resistance in the damaged and undamaged ropes, the latter being only of the order of 1 kΩ, while the former is in the range of several MΩ. Thus, the damage greatly increases the resistance, but it does not block the electrical transport. Obviously, the damaged metallic tubes in direct contact to the gold electrodes carry most of the current, since only a few kΩ would be expected for undamaged nanotubes in the rope, and the semiconducting ones, damaged or undamaged, are insulating. The metallic tubes are one-dimensional systems with two degenerate modes at the Fermi energy [1], hence the resistance of a segment of length $L$ containing defects with an average distance $L_0$ is given by $R = (h/4e^2)(L/L_0)$ (neglecting any interference effects). The extent of the damaged areas along the direction of current transport, i.e., the width of the gold electrodes, is typically 200 nm. (The rope segments between the contacts are undamaged and thus their contribution to the resistance is negligible.) At room temperature, we find resistances of the ropes around 200 kΩ. This resistance corresponds to a mean free path of $L_0 \simeq 6$ nm, which is consistent with the average distance between defects obtained by the Monte Carlo simulation.

In Fig. 1c, both 2t and 4t measurements show an increase in resistance when cooling the sample. This increase is caused by electronic localization in the damaged tube, an interference effect which increases the resistance

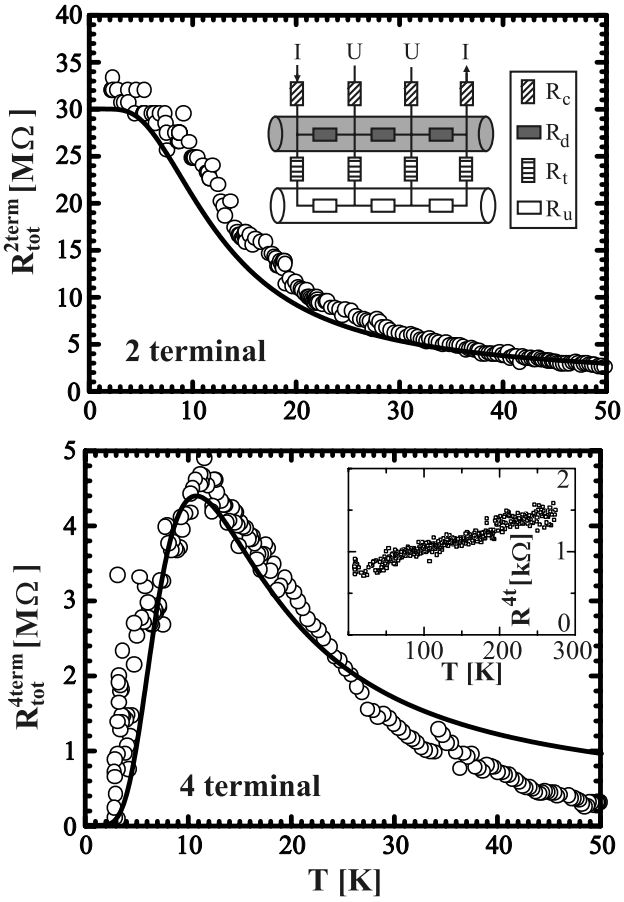


FIG. 2. Comparison between measurement (symbols) and fit (solid line) according to the model described in the text. The insets show the resistance network of the model (upper) and the temperature dependence of the 4t resistance of an undamaged rope (lower). Note the very different resistance scales of the 4t plots.

by coherent backscattering of electrons at the defects. When the phase coherence length exceeds the localization length $ML_0$ ($M$ number of modes) the resistance increases exponentially with decreasing temperature [12].

Below a sample-dependent temperature around 20 K (11 K in the example of Fig. 2), the resistance obtained by the 4t measurement starts to decrease. This effect cannot be caused by some gold-tube contact resistances, since these do not contribute in a 4t measurement. And any scattering mechanism (e.g., phonon scattering), which could possibly lead to such a behavior, would show in both the 4t and the 2t measurement. In general, the absence of a similar decrease in the 2t measurement proves that this behavior cannot be caused by a change in transport inside the actual current path, i.e., the damaged tube. We will now discuss a model of how to understand our experiments and will extract information about tube-tube interactions.

Key to understanding our experiments is the realization that disorder can switch the current path from a tube at the surface to another tube inside the rope. The tubes in the rope are only weakly coupled (corresponding to a large

coupling resistance), so usually one expects the current to be carried by the tube with the lowest contact resistances to the gold electrodes, i.e., a tube at the surface of the rope. In our experiments, the surface tubes (and all other tubes about 6 nm deep into the rope) were damaged during the sputter treatment and thus show high resistance already at room temperature. When the sample is cooled the resistance increases due to localization in the damaged tube, and eventually grows sufficiently high, so that the current switches its path to another undamaged metallic tube deeper inside the rope. This happens when the resistance in the damaged tubes becomes comparable to the large coupling resistance between the tubes. Once this is the case, the current favors the "new" path and switches to the undamaged tube in the bulk of the rope. The model presented in the following paragraph will clarify this behavior.

Consider a network of damaged and undamaged tubes with resistances $R_d$ and $R_u$ ($R_d \gg R_u$), with the intertube coupling resistance $R_t$ and contact resistance $R_c$ which connect the damaged tube at the surface to the gold electrodes. The upper inset in Fig. 2 shows how these resistances are connected in the model. A 2t measurement always detects the two parallel current paths and thus $R^{2t} \approx [(3R_d)^{-1} + (2R_t)^{-1}]^{-1}$, while the 4t measurement is sensitive to whether the main part of the current flows in the surface tube (high temperatures, $R^{4t} \approx R_d$) or in the undamaged "bulk" tube (lowest temperatures, $R^{4t} \approx R_u$). In order to calculate the total 2t and 4t resistances exactly for all temperatures, we have to evaluate the individual resistances. $R_d$ is governed by strong localization and can therefore be described by [12]

$$R_d = \frac{L}{L_\Phi} \frac{h}{2e^2} \frac{1}{2} \left( e^{\frac{2L_\Phi}{ML_0}} - 1 \right).$$

$L_\Phi$ follows a power law dependence on temperature, $L_\Phi \sim T^{-\alpha}$, and we will use this to describe $R_d$. The intertube coupling resistance $R_t$ will be taken to be independent of temperature (we will justify this later on). The coupling resistances are placed underneath the electrodes, i.e., connected to the damaged areas of the surface tube, since a change in current path occurs only where transport inside the surface tube gets "blocked" by localization. The resistance of the undamaged tube $R_u$ is much smaller than $R_t$ and $R_d$ (cf. the lower inset in Fig. 2) and since it is always connected to $R_t$, it does not play any significant role. The last resistance to be discussed is the contact resistance $R_c$ between the gold electrode and the surface tube. This resistance will only show up in 2t measurements but will not contribute to the 4t resistance. We will neglect this resistance for the moment and will justify it later on.

Figure 2 shows experimental data from one of our samples, together with the fits based on our model. The results of both 4t and 2t measurements are well reproduced, underlining the validity of our simple model. First, we note that indeed no additional contact resistances $R_c$ are necessary to describe the 2t measurements. Second, from the fits in Fig. 2 we can extract $L_\Phi(T)$ as a function of temperature. The coherence length turns out to be about 200 nm at the lowest temperature, a value significantly lower than that reported by other groups [6,8,13] since we are dealing with a disordered system. It is well known that disorder significantly enhances phase breaking processes [14]. We find that the temperature dependence of $L_\Phi$ can be described by $L_\Phi \sim T^{-\alpha}$ with $\alpha = 0.33-0.5$. $\alpha = 1/3$ points to dephasing by Nyquist scattering [14], while $\alpha = 1/2$ suggests electron-phonon scattering. Both processes seem to be involved, with the Nyquist scattering possibly becoming dominant at the lowest temperatures [13].

Next we evaluate the coupling resistance $R_t$ between the tubes. $R_t$ is extracted from the data in a very simple manner and turns out to be the most reliable and stable parameter in the simulation, since it is only determined by the *value* of the resistance maximum in the 4t measurement. The temperature dependence of $R_d$ determines the *shape* and *position* of the maximum in temperature [$R_d(T_{\max}) \simeq R_t$]. Since slight variations in sputter damage ($L_0$) significantly affect $R_d$ there is no strict correlation between $R_t$ and $T_{\max}$, but in spite of this $R_t$ can be obtained from the value of the resistance maximum. Analyzing $R_t$ for our 13 samples, we obtained values ranging from 2 to 140 MΩ. Any proposed coupling mechanism must be able to account for this large range of transfer resistance values. Hopping processes are sometimes invoked to describe intertube transport [15]. This mechanism involves transport by hopping through intermediate states (e.g., via other tubes). For our measurements, a single transfer would correspond to a resistance of about 2 MΩ, and thus the highest value of 140 MΩ would need 70 transfers, barely imaginable with only 100 tubes in the rope at all. Moreover, the hopping processes are thermally activated and thus the coupling between tubes would eventually freeze out, leaving the rope insulating at the lowest temperatures, in contrast to the observation. We conclude that the only mechanism that can account for all observations involves tunneling between tubes. In this process a small range of distances between the tubes leads to a large range of resistances due to the exponential dependence typical for tunneling. Furthermore, this process does not freeze out even at the lowest temperatures.

We will now try to link the experimental findings for $R_t$ to the geometry of the rope, i.e., the distances between the bulk and the surface tubes. The cross section of a rope consists of typically 100 single tubes. A fraction of about 2/3 of the tubes is semiconducting, while the remaining 1/3 is said to be metallic [1]. The switching of the current path from damaged to undamaged tubes involves tunneling over some distance $d$ within the triangular lattice of the rope. The depth of the damage of the sputter treatment (about 6 nm) sets a lower limit for the distance $d$ within which an undamaged metallic tube can be found. To describe the

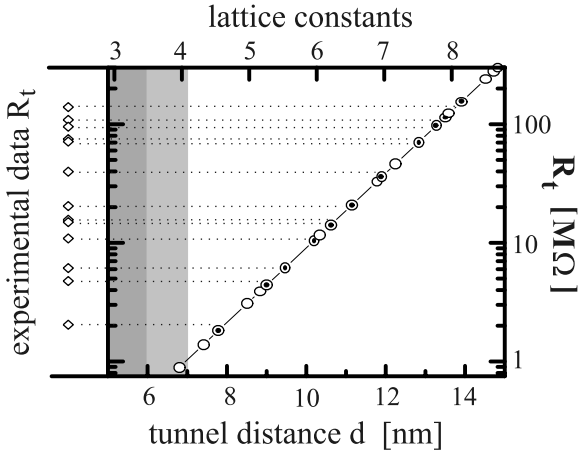


FIG. 3. Comparison between experimentally found coupling resistances $R_t$ (symbols on the left-hand side) and values allowed by the theory (circles) for tunneling between tubes. Filled circles mark coincidences. The shaded area marks the depth of the sputter damage, which sets a lower limit for the observable tunnel distances.

coupling resistance $R_t$ that is caused by the tunnel process, we consider the coupling of two one-dimensional waveguides separated by a tunnel barrier [16]. We thus find that $R_t = (h/4e^2)(v_F/v_\perp)(1/T) \simeq (h/4e^2)e^{2\kappa d}$. The velocity perpendicular to the tube axis $v_\perp$ can be approximated by the Fermi velocity $v_F$ when transport along the damaged tube is blocked by localization. The transmission $T$ in the tunnel process is determined by the overlap of the wave functions of the tubes, with $\kappa$ being related to the barrier height. Given the linear dispersion relation for the metallic nanotubes $\epsilon(k) = \hbar v_F(k - k_F)$ around the Fermi energy and the barrier height $\Phi$, $\kappa$ is calculated as $\kappa = \Phi/(\hbar v_F)$. Since the electrons tunnel through the other tubes, which are mostly semiconducting, the barrier height is given by the conduction band edge of these semiconducting tubes. All nanotubes share the same graphene structure, hence their work function is expected to be nearly the same [7], and the Fermi level of the metallic tubes is expected to align midgap the semiconducting energy gap. With an average band gap of 500 meV we find $\Phi = E_{\text{gap}}/2 \simeq 250$ meV. Using $v_F = 10^6$ m/s [17], we obtain a penetration depth of $1/2\kappa = 1.25$ nm, comparable to the value given in Ref. [18]. Unlike tunneling through vacuum, the low barrier allows for tunneling over large distances between tubes.

Figure 3 compares theoretical and experimental data, where the theoretical predictions result from evaluating the above formula for the discrete distances $d$ realized in the triangular lattice of the rope (the tunnel distance $d$ is the distance between the centers of the involved tubes). We used $\Phi = 225$ meV. Since $k_BT \ll \Phi$, the tunnel resistance is indeed temperature independent. We find that all data points coincide with values allowed by the model. We never did find tunneling into tubes closer than about 8 nm to the damaged surface tube. This is because tunneling into another damaged metallic tube is not favorable. This strongly supports our interpretation. The large variation of tunneling distances from sample to sample is explained by the strong selection rule the tubes have to fulfill for tunneling to be allowed, i.e., the tubes have to have the same chirality [18]. Thus, the theoretical assumption of direct tunneling yields a consistent picture for the electronic coupling in nanotube ropes.

In conclusion, by $Ar^+$ sputtering of single-wall carbon nanotube ropes before making electrical contact to them, defects are introduced that led to strong scattering in the current carrying tubes at the surface of the rope. Below a sample specific threshold temperature the current tunnels into an undamaged, metallic tube in the bulk of the rope, leading to a dramatic reduction of the four terminal resistance. The value of the resistance maximum is related to the intertube coupling resistance between the involved tubes. Using a simple model, this intertube resistance is shown to be caused by direct tunneling between tubes.

[1] R. Saito, M. Fujita, G. Dresselhaus, and M. S. Dresselhaus, Appl. Phys. Lett. **60**, 2204 (1992).
[2] S. J. Tans, A. R. M. Verschueren, and C. Dekker, Nature (London) **393**, 49 (1998).
[3] R. Martel *et al.,* Appl. Phys. Lett. **73**, 2447 (1998).
[4] Z. Yao, H. W. C. Postma, L. Balents, and C. Dekker, Nature (London) **402**, 273 (1999).
[5] J. W. G. Wildöer *et al.,* Nature (London) **391**, 59 (1998).
[6] M. Bockrath *et al.,* Science **275**, 1922 (1997).
[7] M. S. Fuhrer *et al.,* Science **288**, 494 (2000).
[8] S. J. Tans *et al.,* Nature (London) **386**, 474 (1997).
[9] A. Thess *et al.,* Science **273**, 483 (1996).
[10] The simulation was done using the program SRIM, Stopping and Range of Ions in Matter, by J. F. Ziegler and J. P. Biersack.
[11] C. L. Kane *et al.,* Europhys. Lett. **41**, 683 (1998).
[12] S. Datta, *Electronic Transport in Mesoscopic Systems* (Cambridge University Press, Cambridge, 1995).
[13] H. R. Shea, R. Martel, and P. Avouris, Phys. Rev. Lett. **84**, 4441 (2000).
[14] B. L. Altshuler, A. G. Aronov, and D. E. Khmelnitsky, J. Phys. C **15**, 7367 (1982).
[15] A. B. Kaiser *et al.,* Synth. Met. **103**, 2547 (1999).
[16] C. C. Eugster and J. A. del Alamo, Phys. Rev. Lett. **67**, 3586 (1991).
[17] C. Schoenenberger *et al.,* Appl. Phys. A **69**, 283 (1999).
[18] A. A. Maarouf, C. L. Kane, and E. J. Mele, Phys. Rev. B **61**, 11 156 (2000).